2012

Modeling of a Novel Spool Compressor With Multiple Injection Ports

Margaret M. Mathison
margaret.mathison@marquette.edu

James E. Braun

Eckhard A. Groll

Modeling of a Novel Spool Compressor with Multiple Injection Ports

Margaret M. MATHISON[1]*, James E. BRAUN[2], Eckhard A. GROLL[2]

[1]Marquette University, Department of Mechanical Engineering,
Milwaukee, WI, USA
Phone: (414) 288-5650, Fax: (414) 288-7790, margaret.mathison@marquette.edu

[2]Purdue University, School of Mechanical Engineering,
West Lafayette, IN, USA

* Corresponding Author

ABSTRACT

While models have previously been developed to investigate scroll compressor performance with a single injection port, the model described in this paper explores the effect of multiple injection ports on the performance of a novel rotary spool compressor. The model includes the effects of heat transfer and leakage and is numerically solved to predict the compressor power consumption and mass flow rate. The injection ports are modeled assuming that saturated vapor is injected at a specified pressure and the timing of the injection process can be controlled.

Running at a speed of 1907 rpm with R-22 as the working fluid, an evaporating pressure of 391 kPa, an inlet temperature of 7.6°C, and a discharge pressure of 1890 kPa, the model predicts that adding a single injection port will provide a 12% increase in the coefficient of performance (COP) of the cycle. Adding a second injection port increases the COP by an additional 4% compared to the cycle with a single port, or 16% over the baseline performance of the cycle without economization. The compressor model is also used to investigate the effect of injection pressure, injection port location, and injection port diameter on economized cycle performance.

1. INTRODUCTION

Increasing concern over environmental sustainability and energy security motivates continued research to improve the efficiency of vapor compression equipment. Current efforts focus on both improving the efficiency of individual cycle components and exploring modifications to the overall cycle configuration. This paper investigates a novel rotary spool compressor that has been designed with the goal of simultaneously reducing both frictional and leakage losses, which are strong factors impacting rotary compressor performance. In addition, the geometry of the spool compressor makes it relatively easy to add multiple ports for injecting economized refrigerant into the compression pocket. Therefore, the spool design not only addresses the need for more efficient compressors, but also facilitates modifications to the cycle for economizing, which further improves the compressor and cycle performance.

1.1 Novel Rotary Spool Compressor

A traditional rotary vane compressor uses a rotating piston to drive the rotation of a vane that displaces and compresses the working fluid. The compressor relies upon centripetal force to hold the vane in contact with the compressor housing and in some cases uses a spring positioned behind the vane to ensure that it provides sufficient sealing to minimize refrigerant leakage past the vane. However, this results in significant friction at the contact between the vane and housing, which reduces mechanical efficiency and adds to wear. Decreasing the forces acting on the vane to minimize friction results in increased leakage, and this tradeoff limits the compressor performance.

Although similar in design to a rotary vane compressor, the spool compressor developed by Kemp *et al.* (2008; 2010) uses a cam to control the gate motion instead of relying upon centripetal force or a spring to maintain contact between the vane and the housing, which reduces friction losses. The design also aims to reduce friction by rotating the face plates with the rotor, although this creates a new path for leakage between the face plates and the cylinder. However, leakage across the surfaces of the rotor is minimized, and leakage past the gate can also be minimized through proper design of the cam that controls the clearance between the gate and the cylinder.

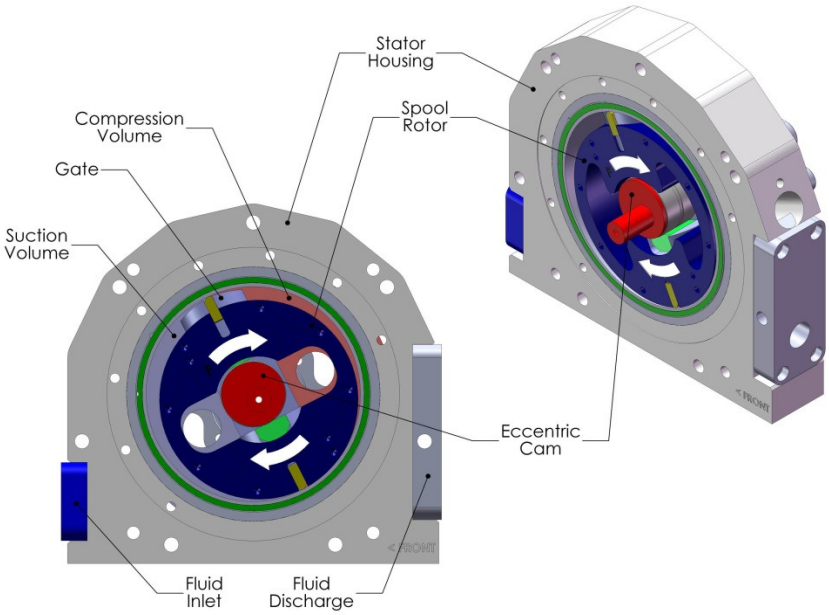

Figure 1: Overview of the spool compressor geometry (Kemp *et al.*, 2010)

Figure 1 shows the inner components of the spool compressor. The spool rotor rotates in the clockwise direction around a stationary axis that is concentric with the driving crankshaft. The stationary housing, with its inner diameter highlighted in green, forms the outer wall of the compression chambers. The cylindrical cam is also stationary and is concentric with the stator. The crankshaft rotation is transmitted both to the gate and the face plates that are attached to the rotor. Figure 2 shows that when these rotating face plates are assembled with the rotor they have the appearance of a spool, which gives the compressor its name.

The results of two experimental studies on the spool compressor have been published. Kemp *et al.* (2008) calculated volumetric efficiencies up to 95% and isentropic efficiencies up to 65% based on the test results for a prototype compressor running with air. An additional study published by Kemp *et al.* (2010) provided test results for a second prototype compressor running with R-134a. The compressor achieved a volumetric efficiency of 98% and an isentropic efficiency of 50% operating at a pressure ratio of 3.5 and a speed of 550 rpm. These initial experimental results show that the spool compressor is capable of achieving high volumetric efficiencies but requires further development to improve the isentropic efficiency. Therefore, the comprehensive compressor model presented in this paper provides a valuable tool for optimizing the compressor design. The spool compressor model will also be used to investigate the impact of multiple injection ports.

1.2 Economized Cycle with Refrigerant Injection

Traditionally, the incorporation of economizing has required the use of a multi-stage compressor, the cost of which has limited the scope of these modified cycles to large-scale applications. Figure 3 shows a common configuration of the economized cycle that uses a flash tank to supply saturated vapor to a mixing point between the compressor stages. The saturated vapor cools the superheated refrigerant exiting the first stage of the compressor, increasing the density at the second-stage inlet and thus reducing the overall compression work per unit mass. Jung *et al.* (1999) extended this concept and used an experimentally validated model to show that a cycle with three-stage compression and two economizers has a higher COP than a cycle with two-stage compression and one economizer. Mathison *et al.* (2011) used a cycle model to estimate the additional performance improvements that could be achieved

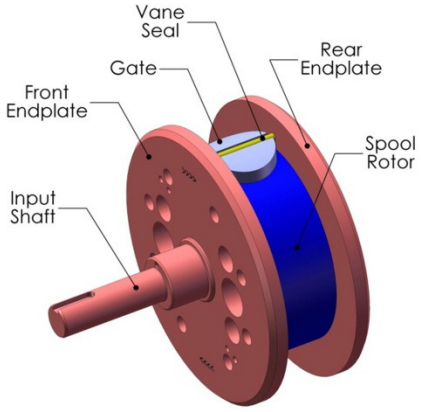

Figure 2: Spool assembly formed by the face plates and rotor (Kemp *et al.*, 2010)

with further staging and injection of two-phase economized refrigerant. However, increasing the number of stages substantially increases the compressor cost and complexity. Injection ports, which can be used to provide cooling by injecting economized refrigerant during the compression process, provide a relatively simple and inexpensive alternative to multi-stage compressors

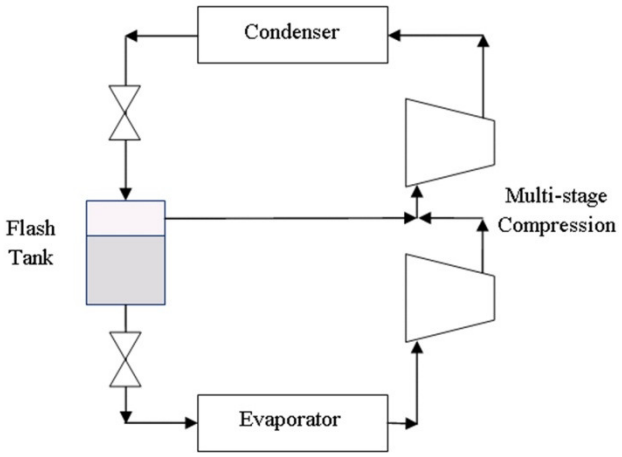

Figure 3: Vapor compression cycle with two-stage compression and flash-tank economization

Previous research on refrigerant injection ports has focused on their application in the scroll compressor. The scroll compressor with a single injection port for vapor injection has been patented (Perevozchikov, 2003) and is marketed as a tool for increasing system capacity and system efficiency. Dutta *et al*. (2001), Park *et al*. (2002), Winandy and Lebrun (2002), and Yamazaki *et al*. (2002) have all explored techniques for modeling the scroll compressor with liquid or vapor injection. One of the most comprehensive models, developed by Wang *et al.* (2008), considers both liquid and vapor injection and applies separate mass and energy balances to the liquid and vapor phases assuming that the pressure and temperature of the liquid and vapor phases remain equal. The model is validated using experimental results and is integrated into a system level model to investigate the effects of injection pressure, port size, and port location on performance (Wang *et al.,* 2009b). The optimum operating conditions for maximizing capacity and COP are also investigated (Wang *et al*., 2009a).

While the models of the scroll compressor with one vapor injection point developed by Wang *et al.* and Dutta *et al.* are fairly comprehensive, the current work aims to characterize the performance of the spool compressor with multiple injection points. Mathison (2011) predicts comparable improvements in COP with either vapor or two-phase injection, and thus the spool compressor model considers only vapor injection to limit the system complexity.

2. MODEL DEVELOPMENT

2.1 Geometry Model

Figure 4 shows a simplified cross-section of the spool working chambers in a plane centered between the two face plates, where the width of the cylindrical gate is equal to its diameter. In this figure the gate rotates in the clockwise direction; the gas enters through an open suction pipe located to the right of top dead center and exits through a discharge port with a reed valve located to the left of top dead center. The two gate tips act as boundaries between chambers in the compressor. A third boundary is formed by the point of minimum clearance between the rotor and stator, which will be referred to as top dead center (TDC). The three working chambers in Figure 4 are identified as the suction, compression and discharge chambers. The gate position is fixed by the crankshaft angle, θ, measured in the direction of rotation for the crankshaft.

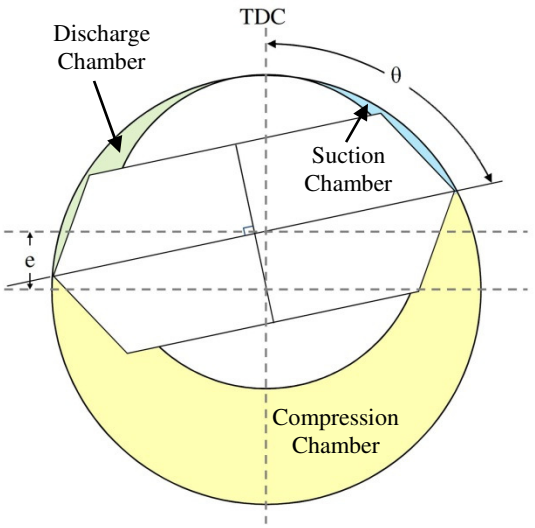

Figure 4: Overview of the spool compressor identifying the suction, compression and discharge chambers

The volume and surface area of each chamber can be calculated as a function of crankshaft angle by developing equations to describe the chamber boundaries, as detailed by Mathison (2011). The resulting plot of chamber volume versus crankshaft angle in Figure 5 shows that each chamber undergoes two identical processes over the course of one crankshaft rotation. At the end of the first suction process,

the volume trapped between the two gate tips becomes the compression chamber. The volume of the compression chamber continues to increase until it reaches a maximum value approximately halfway through the compression process. The gas contained in the compression chamber at the end of the compression process then becomes the discharge volume.

The effect of the gate on the chamber volume is most noticeable at the beginning and end of the suction and discharge processes, when the gate tip approaches TDC. Near TDC the gate actually recedes below the surface of the rotor, and thus the gate slot adds to the volume of the suction and discharge chambers. As the gate slot moves past TDC, its volume shifts from impacting the discharge chamber to impacting the suction chamber. However, once the edge of the gate moves past TDC, the fraction of the gate slot that impacts each chamber no longer changes. This results in a slight discontinuity at a crankshaft angle of approximately 20.7°C, when the edge of the gate passes TDC.

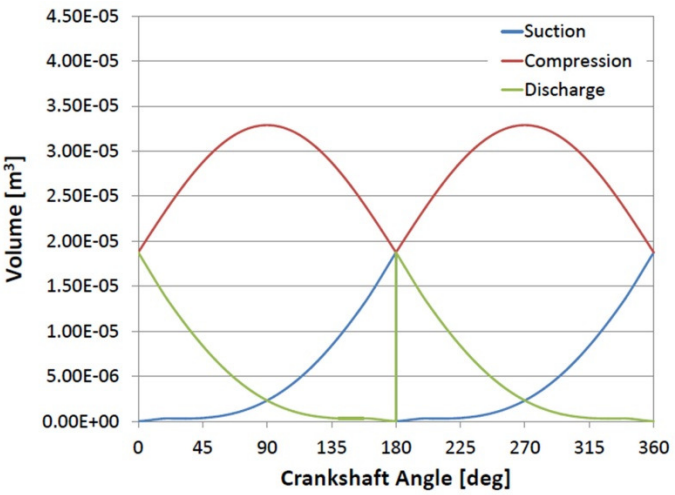

Figure 5: Volume of the suction, compression and discharge chambers over one crankshaft rotation

2.2 Compression Process Model

A thermodynamic model of the compression process is developed by applying mass and energy balances to each of the control volumes in the compressor, including the suction, compression and discharge chambers. Solving these conservation equations requires estimates of the refrigerant leakage flow rates between control volumes and the heat transfer rate between the cylinder wall and the refrigerant by convection. However, the leakage and heat transfer rates depend upon the conditions in the control volumes, which are initially unknown, and thus solving the mass and energy balances is an iterative process. Numerical methods are used to predict the pressure and temperature variations over one rotation of the crankshaft, and the compressor power input, the refrigerant mass flow rate, and the compressor efficiencies can be calculated based upon these profiles. Many examples of compressor models that follow this development process are available (Bell., 2011; Bradshaw *et al.*, 2010; Mathison *et al.*, 2008; Mathison, 2011), and therefore the details of deriving and solving the conservation equations are not presented in this paper.

2.3 Injection Model

The mass flow through the injection ports is modeled as isentropic flow of a compressible ideal gas. The model requires the user to specify the number of ports to be considered, the diameter of each port and the crankshaft angle at which the gate tip reaches each injection port. In addition, the user must specify the pressure in each injection line, which is assumed to remain constant with respect to time.

The injection model also assumes that the timing of the injection process can be controlled. In practice, this would require a small actuated valve similar to those used to achieve variable valve timing in internal combustion engines, which may prove difficult to implement. However, assuming that such a solution exists provides the most flexibility in evaluating the effects of injection over a wide range of conditions.

The length of the injection process is selected to maintain steady-state conditions in the cycle when the phase separator supplies saturated vapor to the injection line and saturated liquid to the next expansion valve. Therefore, the quality of the refrigerant entering the flash tank determines the fraction of the total mass flow rate that must run through the injection line. Under steady-state conditions, the average mass flow rate of refrigerant supplied to the injection lines must match the time-averaged mass flow rate of vapor through the injection ports. The residual difference between these two quantities is used to adjust the timing of the injection process until the mass flow rates converge.

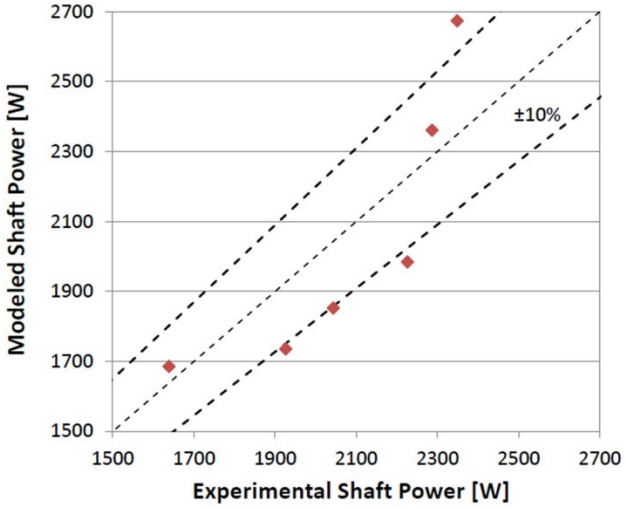

Figure 6: Comparison of predicted and measured power consumption of the spool compressor at six operating conditions

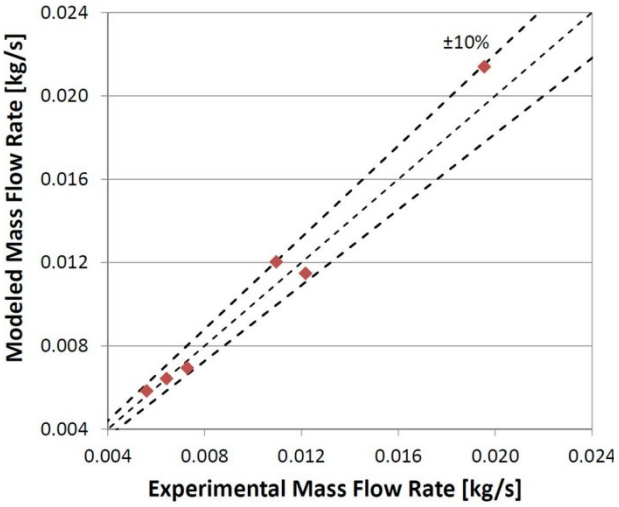

Figure 7: Comparison of predicted and measured refrigerant mass flow rate through the spool compressor at six operating conditions

3. RESULTS AND DISCUSSION

3.1 Comparison of Modeled and Experimental Results without Injection

External tests of a prototype spool compressor without injection were conducted using a Tescor calorimeter. However, an additional test stand located adjacent to the calorimeter was needed to accommodate the compressor, motor and oil management system, and thus the tests were not conducted in the temperature-controlled chamber.

Several of the model parameters were tuned to improve the correlation between modeled and experimental results. The mass fraction of mineral oil that enters the compressor has a significant impact on the temperature at the compressor exit due to its high specific heat capacity and density. However, the mass flow rate of oil was not measured in the experiments. Therefore, the estimated oil mass fraction was tuned to a value of 44.5% in the model to achieve agreement between the measured and modeled discharge temperatures.

Similarly, the mechanical efficiency of the compressor was tuned to a value of 40% based on the compressor power consumption. Figure 6 shows that the modeled power consumption agrees within ±11% of the experimental values. However, the assumption that mechanical efficiency remains constant over the entire range of operating conditions causes the model to underpredict the power consumption at high pressure ratios, which increase the imbalance of forces acting on the gate and spool, and overpredict the power consumption at low speeds. While five of the experimental tests were conducted at the same speed, the case with the lowest power consumption in Figure 6 corresponds to the test condition at which the compressor was operated at a lower speed.

Finally, the refrigerant mass flow rate through the compressor was tuned by varying the flow coefficients on the leakage paths; the mass flow rates across the gate tips were multiplied by a factor of 1.15, while the mass flow of leakage between the rotor and the stator at TDC was multiplied by a factor of 0.49. Figure 7 shows that the model and experimental mass flow rates agree within ±10%.

The tuned model provides a tool for analyzing the compressor performance both with and without vapor injection. Although the model was tuned using experimental results without vapor injection, it is assumed that the tuned parameters will not change significantly with the incorporation of injection.

3.2 Model Results with One Injection Port

Figure 8 plots the pressure variations with crankshaft angle in the suction, compression and discharge chambers when the compressor operates both with and without injection. The operating conditions include an evaporating

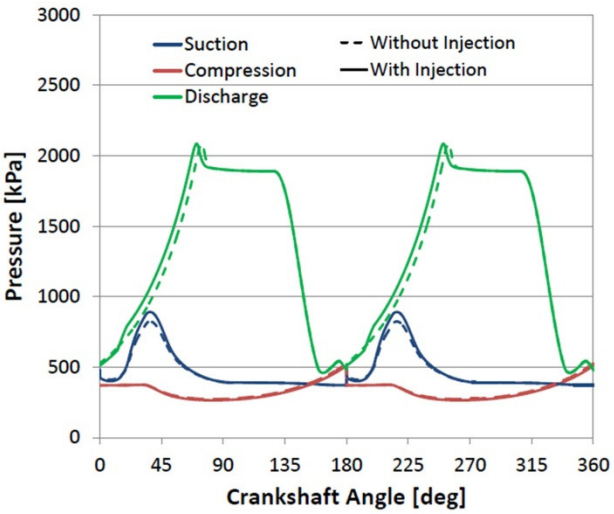

Figure 8: Comparison of working chamber pressures for the spool operating with and without vapor injection at Test Condition 3. The 1.27-cm-diameter vapor injection port, located at 230°, supplies saturated vapor at 800 kPa

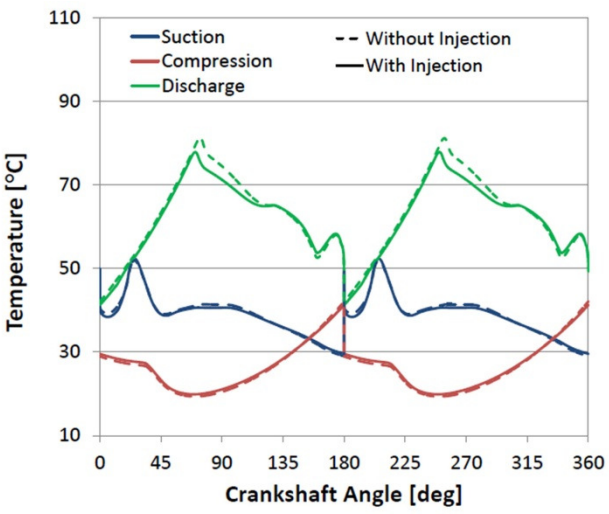

Figure 9: Comparison of working chamber temperatures for the spool operating with and without vapor injection at Test Condition 3. The 1.27-cm-diameter vapor injection port, located at 230°, supplies saturated vapor at 800 kPa

temperature of -7.2°C, a suction temperature of 7.6°C and a condensing temperature of 48.8°C. With R-22 as the working fluid, this corresponds to a suction pressure of 390.9 kPa and a discharge pressure of 1889.1 kPa. This operating condition will be referred to as "Test Condition 3" for the purposes of this paper.

At the beginning of the suction process the volume of the suction chamber is very small and the chamber is not open to the suction port. Therefore, flank leakage from the discharge chamber initially causes a noticeable rise in the suction chamber pressure, which drops again once the chamber opens to the suction port. The compression chamber remains open to the suction port and the chamber volume increases during the first half of the compression process, but the pressure begins to gradually increase once the gate tip passes the suction port and the chamber is sealed. The pressure continues to increase during the discharge process until the valve opens and then remains fairly constant until the valve closes again. Once the valve closes, the pressure drops due to leakage to the suction and compression chambers, which decreases the mass of refrigerant remaining in the small discharge volume.

Leakage will affect not only the pressure, but also the temperature and density in each control volume. Figure 9 shows the variations in the suction, compression and discharge chamber temperatures over one crankshaft rotation. The suction chamber temperature increases quickly due to the high temperature of the gas leaking into the chamber through the clearance at top dead center. However, the temperature begins to drop once the chamber opens to suction pipe and continues to decrease during the first half of the compression process due to both the flow through the suction pipe and the increasing chamber volume. The temperature in the discharge chamber increases until the valve opens and then begins to drop as flow exits through the discharge port.

When the model runs with vapor injection, the pressure difference between the refrigerant in the injection line and in the chamber where the port is located will drive the injection process. The model assumes that an idealized valve is able to control flow through the injection port based on this pressure difference. The valve allows flow through the injection port when the driving pressure difference at the port falls within a particular range of pressures but otherwise remains closed to prevent backflow to the injection line and to limit the amount of vapor injected into the compressor. As discussed previously, the range of pressures over which the injection process occurs is determined such that the mass flow rate of vapor injected into the compressor balances the mass flow rate of vapor generated during the expansion process. Figure 10 plots the injected mass flow rate as a function of crankshaft angle when saturated vapor at 800 kPa is supplied to one injection port with a diameter of 1.27 cm. The injection port is located such that the gate tip reaches the port at a crankshaft angle of 230°, and thus the injection port is open to the

discharge chamber for the majority of the rotation. The first pulse of injected vapor enters the discharge chamber at a crankshaft angle of approximately 13° and the flow continues for slightly over 7° of crankshaft rotation.

The effect of the injection flow on the pressure in the working chambers can be seen in Figure 8. Because the injection pressure is greater than the pressure in the discharge chamber, the injection process raises the pressure in the discharge chamber. The slightly higher pressure in the discharge chamber also increases leakage into the suction chamber through the clearance between the rotor and the stator, which is reflected by an increase in the suction chamber pressure when the suction volume is small and leakage has the greatest impact.

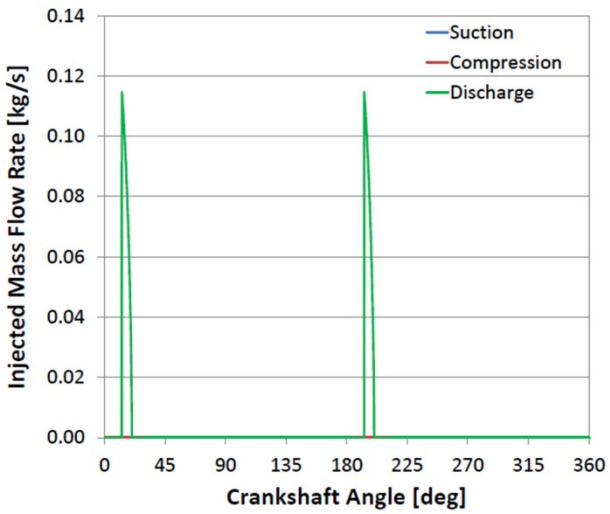

Figure 10: Mass flow rate through the injection port for the spool operating at Test Condition 3. The 1.27-cm-diameter injection port, located at a crankshaft angle of 230°, supplies saturated vapor at 800 kPa

Figure 9 shows that the effect of injection on the temperatures in the working chambers is more subtle, resulting in a slight shift to lower temperatures without any discontinuity marking the beginning of the injection process. The refrigerant enthalpy in the discharge chamber will experience a marked decrease due to the vapor injection, which acts to decrease the chamber temperature. However, the increase in chamber pressure that accompanies injection offsets this effect, resulting in a smooth temperature variation despite the injection process. The most significant reduction in temperature with injection is seen at the beginning of the discharge process; the higher pressure in the discharge chamber with injection causes the discharge valve to open earlier in the crankshaft rotation, when the discharge temperature is noticeably lower. The effect of injection on the suction and compression chamber temperatures is relatively minor.

To measure the impact of injection on compressor power consumption, a normalized power consumption is defined as the ratio of the modeled power consumption with injection to the modeled power consumption without injection. The impact of injection on the cycle's cooling capacity is equally important, and therefore the model estimates the capacity of the cycle assuming that refrigerant exits the condenser as a saturated liquid. The normalized cooling capacity is defined as the ratio of the cycle capacity with injection to the unmodified cycle capacity.

Figure 11 plots the normalized power consumption and cooling capacity over a range of injection pressures when the location and diameter of the injection port remain unchanged. For the specified port parameters, a maximum reduction in power consumption of 11.0% occurs with an injection pressure of approximately 900 kPa. While an intermediate pressure of 860 kPa would provide equal pressure ratios across the stages of a two-stage compressor and would minimize its power consumption, the model with refrigerant injection predicts a higher optimum injection pressure due to the increased mass flow rate through the compressor following injection.

The cooling capacity of the cycle decreases slightly with refrigerant injection due to the reduction in mass flow through the evaporator. In a cycle operating without superheat at the compressor inlet, drawing off refrigerant that has already evaporated to be used for injection would have no detrimental effect on the cooling capacity (Mathison, 2011). However, the results in Figure 11 correspond to an operating condition with significant superheat, in which case the energy absorbed by the refrigerant as it is heated from the saturated vapor to the superheated vapor state contributes to the cooling capacity of the cycle. Therefore, the reduction in mass flow through the evaporator results in a slightly lower cooling capacity compared to the cycle without injection.

Nonetheless, the reduction in power consumption provided by vapor injection outweighs the loss of cooling capacity to result in a net improvement in COP. Figure 12 presents the COP of the cycle with injection relative to the cycle without injection; the results are calculated for the same injection port size used in Figure 11 with multiple possibilities for the port location. For a port located at an angle of 230° the power consumption was minimized with an injection pressure of approximately 900 kPa, but the COP is maximized at a slightly higher injection pressure.

With an injection pressure of 1100 kPa, the model predicts that saturated vapor injection will increase the cycle COP by 11.7%. The model also predicts that the performance benefits drop off sharply at higher injection pressures, which suggests that the cycle should be designed to err towards lower injection pressures.

The results are also plotted for cases when the injection port is located at 275° and 330°. When the port is located at an angle of 230° or 275° it is initially open to the discharge chamber and supplies a pulse of injected mass flow that only impacts the discharge chamber once in every 180° of rotation. However, moving the injection port to higher angles results in a second pulse of refrigerant that is injected into the discharge chamber as the pressure drops after the discharge process. Injecting refrigerant into the clearance volume that remains after the discharge port closes provides no benefits and reduces the mass flow rate of refrigerant that can be injected during the first pulse. Therefore, the benefits of injection are less substantial if the injection port is located too close to the discharge port. These factors suggest that the port should be located at lower crankshaft angles.

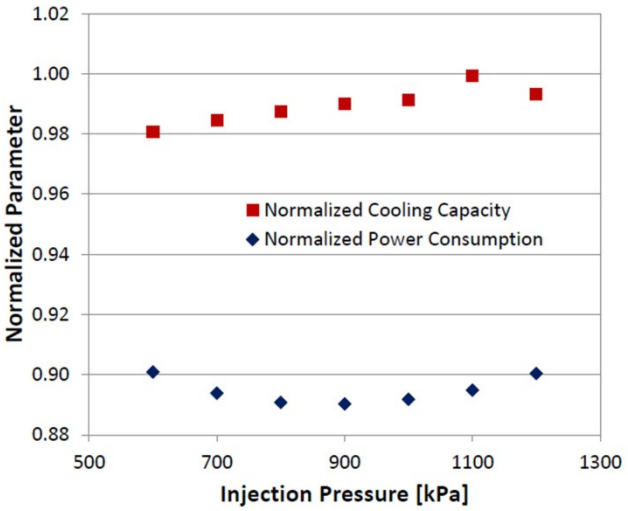

Figure 11: Normalized power consumption and cooling capacity for a cycle using the spool with vapor injection at Test Condition 3. The 1.27-cm-diameter vapor injection port is located at 230°

However, moving the injection port to lower angles can have detrimental effects as well. For example, moving the port to lower angles can reduce or eliminate the amount of time that the injection port is open to the discharge chamber, which can result in larger pressure differences driving the injected flow. Because the difference in refrigerant enthalpies between the injection line and the gas in the chamber decreases as the pressure difference increases, this has a detrimental effect on the cooling benefits of injection. In addition, moving the injection port to lower angles increases the probability of injected refrigerant flowing back through the suction pipe.

The final parameter that affects compressor performance with vapor injection is the port diameter. The mass flow rate through the injection port, which determines the period of time that the port must remain open, is proportional to

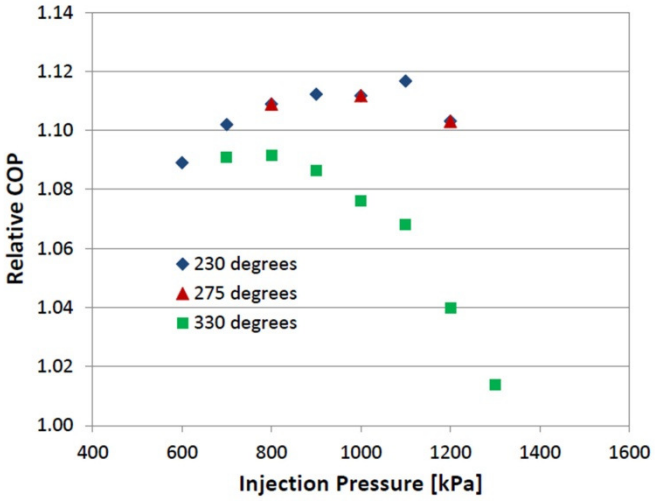

Figure 12: Effect of injection pressure on normalized cooling COP of a cycle using the spool with a 1.27-cm-diameter vapor injection port at Test Condition 3

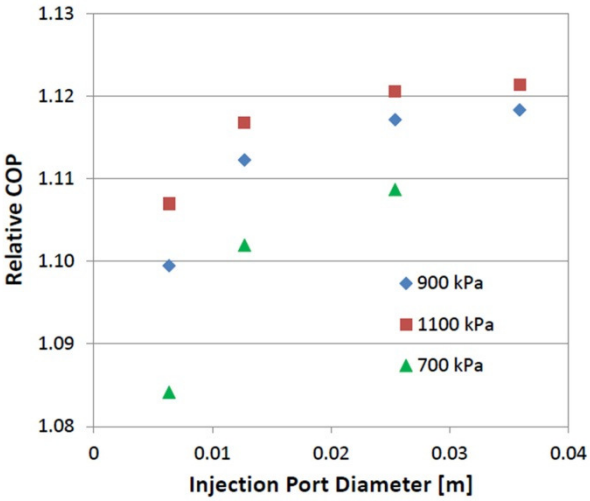

Figure 13: Effect of port diameter on normalized cooling COP of a cycle using the spool at Test Condition 3 with a vapor injection port at 230°

the square of its diameter. If the port diameter is too small, then the injection process requires more time and begins while the refrigerant in the working chamber is at a lower enthalpy, limiting the cooling effects of injection. While increasing the size of the injection port will increase leakage flow rates past the port if the valve that seals the port is not flush with the stator surface, the current model assumes that there is no clearance volume between the valve and stator surface. Therefore, Figure 17 shows that the model predicts that increasing the port diameter only serves to improve the cycle COP. The plot also shows that the cycle performance becomes slightly less sensitive to port diameter at higher injection pressures due to lower mass flow rates through the injection ports.

Of the combinations of injection line pressures, port diameters and port locations investigated, the best performance was achieved with an injection pressure of 1100 kPa and a port with a diameter of 3.59 cm located at 230°. However, because this excessively large port would be impractical to implement, the remaining discussion focuses on an injection port with a diameter of 1.27 cm.

Table 1: Comparison of model results for spool compressor at Test Condition 3 with and without vapor injection

	Two Injection Ports	One Injection Port	Without Injection
First Injection Port			
Port Diameter [cm]	1.27	1.27	
Port Location	190	230	
Injection Pressure [kPa]	700	1100	
Injection Temperature [C]	10.9	27	
Flash Tank Quality	0.12	0.16	
Second Injection Port			
Port Diameter [cm]	1.27		
Port Location	270		
Injection Pressure [kPa]	1200		
Injection Temperature [C]	30.3		
Flash Tank Quality	0.14		
Discharge Temperature [C]	70.7	71.8	74.3
Power Consumption [kW]	2.51	2.44	2.38
Normalized Power	0.85	0.89	1
Mass Flow Rate [kg/hr]	53.4	49.7	43.3
Overall Isentropic Efficiency	21.5%	21.4%	21.8%
Volumetric Efficiency	58.8%	54.7%	47.8%
COP	0.878	0.847	0.758
Normalized COP	1.16	1.12	1

4.3 Model Results with Two Injection Ports

Optimizing the compressor design proves more challenging with two injection ports. As a starting point for designing a compressor with two ports, injection pressures of 700 kPa and 1200 kPa were selected to approximately balance the pressure ratios across the system. The ratio of the low injection pressure to the suction pressure is 1.8, while the ratio of the high and low injection pressures is 1.7 and the ratio of the discharge pressure to the high injection pressure is 1.6. Based on the observations with one injection port, the slight decrease in the pressure ratio as the mass flow rate through the compressor increases is expected to improve the compressor performance.

Table 1 compares the model results obtained with two 1.27-cm diameter injection ports operating at these pressures to the maximum performance of the compressor with one 1.27-cm diameter injection port and without injection. As was expected, the model predicts that increasing the number of injection ports decreases the compressor power consumption per unit mass flow through the condenser. While one injection port decreases the specific power consumption by 11%, adding the second port provides an additional 4% decrease in specific power. This results in a 12% increase in COP with one injection port, or a 16% improvement over the baseline cycle COP with two ports. The volumetric efficiency also increases as the injection ports are added, but the isentropic efficiency, calculated by assuming that the suction stream and injection stream are compressed in parallel, remains relatively constant.

6. CONCLUSIONS AND RECOMMENDATIONS

A model of a novel rotary compressor has been developed and validated. The model predicts the mass flow rate through the compressor within ±10% of experimental values, and predicts the compressor power consumption within ±11% of experimental values.

A single injection port was added to the compressor model and was used to study the effect of port diameter, location and injection pressure on compressor performance. Integrated with a simple cycle model, the compressor

model predicted the greatest improvement in cycle COP when the injection pressure was slightly above the injection pressure that would result in equal pressure ratios across the system. The compressor performance does not vary significantly with the position of the port for injection ports located between approximately 200° and 300°. However, if the injection port is located too close to the discharge port, then injection can occur into the clearance volume. Increasing the injection port diameter has a relatively small influence on performance unless the compressor operates with a low injection pressure.

The addition of a second injection port further reduced the specific power consumption of the compressor, increasing the cycle COP. For an R-22 cycle operating with an evaporating temperature of -7.2°C, a suction temperature of 7.6°C and a condensing temperature of 48.8°C, the model predicted that one injection port would increase the cycle COP by 12%, while a second port increased the COP by 16% compared to the base case.

Further work is needed to develop practical solutions for controlling both the injection flow into the compressor and the flash tanks, which must operate at multiple injection pressures and under transient conditions. However, the reduction in power consumption possible through economization, particularly with multiple injection ports, justifies further work to overcome these challenges.

REFERENCES

Bell, I., *Theoretical and experimental analysis of liquid flooded compression in scroll compressors*, Dissertation, Purdue University, West Lafayette: ProQuest/UMI, Publication No. AAT 3475393.

Bradshaw, C., Groll, E., Garimella, S., 2011, A comprehensive model of a miniature-scale linear compressor for electronics cooling, *Int. J. Refrig.*, vol. 34, no. 1: p. 63-73.

Dutta, A. K., Yanagisawa, T., Fukuta, M., 2001, An investigation of the performance of a scroll compressor under liquid refrigerant injection, *Int. J. Refrig.*, vol. 24, no. 6: p. 577-587.

Jung, D., Kim, H., Kim, O., 1999, A study on the performance of multi-stage heat pumps using mixtures. *Int. J. Refrig.*, vol. 22, no. 5: p. 402-413.

Kemp, G., Garrett, N., Groll, E., 2008, Novel rotary spool compressor design and preliminary prototype performance, *Proc. Int. Compres. Eng. Conf. at Purdue*, p. 1328.

Kemp, G., Elwood, L., Groll, E., 2010, Evaluation of a prototype rotating spool compressor in liquid flooded operation, *Proc. Int. Compres. Eng. Conf. at Purdue*, p. 1389.

Mathison, M., Braun, J., Groll, E., 2008, Modeling of a two-stage rotary compressor, *HVAC&R Res.*, vol. 14, no. 5: p. 719-748.

Mathison, M., Braun, J., Groll, E., 2011, Performance limit for economized cycles with continuous refrigerant injection, *Int. J. Refrig.*, vol. 34, no. 1: p. 234-242.

Mathison, M., 2011, *Modeling and evaluation of advanced compression techniques for vapor compression equipment*, Dissertation, Purdue University, West Lafayette: ProQuest/UMI, Publication No. AAT 3481099.

Park, Y. C., Kim, Y., Cho, H., 2002, Thermodynamic analysis on the performance of a variable speed scroll compressor with refrigerant injection, *Int. J. Refrig.*, vol. 25, no. 8: p. 1072-1082.

Perevozchikov, M., 2003, Scroll compressor with vapor injection, U.S. Patent 6,619,936.

Wang, B., Shi, W., Li, X., Yan, Q., 2008, Numerical research on the scroll compressor with refrigeration injection, *Appl. Therm. Eng.*, vol. 28, no. 5-6: p. 440-449.

Wang, B., Shi, W., Han, L., Li, X., 2009a, Optimization of refrigeration system with gas-injected scroll compressor, *Int. J. Refrig.*, vol. 32, no. 7: p. 1544-1554.

Wang, B., Shi, W., Li, X., 2009b, Numerical analysis on the effects of refrigerant injection on the scroll compressor, *Appl. Therm. Eng.*, vol. 29, no. 1: p. 37-46.

Winandy, E.L., Lebrun, J., 2002, Scroll compressors using gas and liquid injection: experimental analysis and modeling, *Int. J. Refrig.*, vol. 25, no. 8: p. 1143-1156.

Yamazaki, H., Itoh, T., Sato, K., Kobayashi, H., Kawada, M., 2002, High performance scroll compressor with liquid refrigerant injection, *Proc. Int. Compres. Eng. Conf. at Purdue*, p. C22.

ACKNOWLEDGEMENT

The authors would like to acknowledge the support of Mr. Greg Kemp, founder and CTO of Torad Engineering, and Mr. Joe Orosz, President of Torad Engineering.